

## A time-dependent approach to conductance in narrow channels

This article has been downloaded from IOPscience. Please scroll down to see the full text article.

1993 J. Phys.: Condens. Matter 5 L289

(<http://iopscience.iop.org/0953-8984/5/20/001>)

View [the table of contents for this issue](#), or go to the [journal homepage](#) for more

Download details:

IP Address: 171.66.16.159

The article was downloaded on 12/05/2010 at 14:03

Please note that [terms and conditions apply](#).

## LETTER TO THE EDITOR

# A time-dependent approach to conductance in narrow channels

K Stratford and J L Beeby

Department of Physics and Astronomy, University of Leicester, University Road, Leicester LE1 7RH, UK

Received 1 March 1993, in final form 30 March 1993

**Abstract.** An application of the time-dependent Schrödinger equation to the numerical evaluation of the conductance of a quantum point contact is described. For this purpose a single electron at zero temperature is represented by a Gaussian wave packet. Results are presented for a simple point contact geometry with a smoothly varying confining potential. The flexibility in choice of the model potential could make the approach suitable for a wider range of similar problems.

A common approach to dynamical problems in quantum mechanics is to evaluate the elements of the scattering matrix for the time-independent Schrödinger equation. To this end the full wave function must be approximated as a combination of a finite number of (often plane wave) basis states. The accuracy of the calculation will then depend essentially upon this number being sufficiently large. For physical problems in which the potential is of a complicated form, such as an atom or molecule scattering from a surface, the number of basis states required in the expansion of the wave function can become very large. The numerical effort then required either to diagonalize the Hamiltonian for the problem (a process which scales as the cube of the number of basis states) or to evaluate the transfer matrices can become impractical when only limited computational resources are available. For this reason it is of some interest to consider methods which can give useful results without recourse to demanding numerical calculations on large machines.

For physical problems in which it is desirable to study the effect of a realistic model potential the alternative of a time-dependent approach may be adopted. This is of particular value in the case of ballistic transport in quantum wires where the exact geometry and form of the potential defining the constriction has proved to be very important. Time-dependent methods can offer the advantage of allowing problems which may be computationally expensive or difficult in terms of a scattering matrix calculation to be performed in a simple, but effective and efficient manner.

The integration of the time-dependent Schrödinger equation (TDSE) can be implemented by means of highly optimized Fourier transform methods which allow the application of the individual operators appearing in the Hamiltonian in the representation in which they are diagonal. A number of propagation schemes are available at the present time (for a review of time-dependent methods see, for example, [1]). It is the purpose of this letter to illustrate the method by describing its use for the evaluation of the conductance of a quantum point contact in two dimensions and present the results for three simple model potentials.

Transport problems in mesoscopic systems are often treatable in a single-electron calculation by adopting an effective mass Hamiltonian

$$\mathcal{H} = -(\hbar^2/2m^*)\nabla^2 + V_{\text{ext}}(x, y) \quad (1)$$

where  $V_{\text{ext}}(x, y)$  is the two-dimensional artificial potential landscape in which the electron is forced to move. A GaAs effective mass of  $m^*=0.067$  is used for the present calculations. Since the first reports [2, 3] of the quantization of point contact conductance in integer units of the quantity  $2e^2/h$ , a number of calculations have been performed for various geometries and confining potentials [4–9]. Typical is the so-called wide–narrow–wide geometry in which the point contact is defined by abrupt changes in the width of a hard wall potential. The use of an abruptly changing potential causes the appearance of artificial ‘organ-pipe’ resonances in the familiar conductance staircase which arise from strong reflections from the ends causing interference between left- and right-going waves. If the wave function is allowed to evolve adiabatically [10] in the presence of a potential smooth on the scale of the Fermi wavelength such interference is not expected. Indeed, calculations involving a smoothly varying confining potential [11] do not exhibit resonance structure. This is in accord with typical experimental observations at low temperatures where one does not expect see such features.

The integration of the TDSE is an initial value problem in contrast to the boundary value problem presented by the calculation of the scattering matrix. This requires that a suitable, spatially localized, initial wave function must be chosen. The problem is set up on a discrete rectangular grid made up of a total of  $N$  points. For the calculations presented here a standard normalized Gaussian wave packet with circular symmetry is selected:

$$\Psi(x, y; t = 0) = [2\pi\delta^2]^{-1/2} e^{-(x-x_0)^2/4\delta^2} e^{ik_x x} e^{-(y-y_0)^2/4\delta^2} e^{ik_y y}. \quad (2)$$

This wave packet has a finite width in both real and momentum space, the width in real space being set by the parameter  $\delta$  which is subject to two constraints in these calculations. First, the wave packet should not be so wide in momentum space that significant spreading occurs in real space during the time of interest. The second condition on  $\delta$  is that the width of the packet in real space must be large enough that it does not pass straight through the point contact as a classical particle. It is clear that these two conditions on the size of the wave packet are not incompatible. In practice, the width  $\delta$  is taken to be a factor of approximately three or four times greater than the width of the point contact. The energy of the wave packet is taken to be free-electron-like with the wave vector equal to the central component of the momentum space packet  $k = (k_x, k_y)$ . This assumes that the internal energy of the wave packet is negligible. The effect of the spread of energies in the wave packet (which is not assumed to be negligible) on the results is discussed later.

The general form of the artificial confining potential  $V_{\text{ext}}(x, y)$  is parabolic in the  $y$ -direction and has its width smoothly varied at the ends to provide a non-abrupt geometry. The nominal width of the point contact is taken to be twice the classical turning point of the harmonic oscillator ground state at the middle of the constriction. The initial wave function (2), initially placed in a region of zero potential, is propagated through the potential until such a time as the transmitted and reflected portions of the packet are clearly resolved. The transmission coefficient for given incident wave vectors can then be evaluated by means of a numerical integration of  $|\Psi(x, y, t_{\text{fin}})|^2$  over that part of the grid containing the transmitted fraction of the wave packet. Alternatively, the transmission may be obtained by calculating the total probability flux passing through the point contact after each time step of the

propagation and calculating the total at the end of the simulation by means of an integration over time. The latter method allows the use of a smaller grid and is employed for these calculations. The propagation scheme due to Fleck *et al* [12, 13], which is a many-step scheme, is utilized for this purpose. The numerical cost of calculation scales as  $N \log N$  (from fast Fourier transform) multiplied by the number of time steps required (inversely proportional to the group velocity of the wave packet).

The value of the transmission coefficient will clearly be dependent upon the direction of motion of the wave packet when it strikes the opening of the channel. In order to evaluate the conductance of the point contact the transmission is calculated for a number of incident directions. This quantity, weighted by a factor of  $(k_x)^{-1}$  is integrated over all incoming directions in a process which is equivalent to calculating the conductance with the two-terminal Landauer formula [14]. The effect of the wave packet is included by the introduction of a factor related to the flux incident on the channel. Details of this part of the calculation will appear elsewhere [15]. However, it should perhaps be stressed here that only a small number of simulations are required for the calculation of the conductance for a given wave packet energy, the contribution to the total being very small for shallow angles of incidence compared to that from more 'head-on' incidence.

The calculation of the conductance as a function of the wave packet energy has been carried out for fixed point contact width on a grid of  $512 \times 128$  points. The nominal width of the channel for the results shown in figure 1 was approximately 40 Å. Three different channels with length-to-width ratios of 3:1, 5:1, and 10:1 are considered, all exhibiting the familiar conductance staircase. The accuracy of the quantization in units of the fundamental  $2e^2/h$  is good to approximately 1–2%. It is clear from the figure that quantization is better defined for the longer channels, a fact that may be explained simply in terms of the time that the wave function has to experience the potential. The improvement in the quality of the quantization with length-to-width ratio is well documented (see, for example, [6, 7]). As the sides of the confining potential are smooth on the scale of the electron wavelength, the wave function is allowed to move into the constriction adiabatically with no extra structure due to resonances arising. However, some broadening of the conductance steps will have taken place due to the energy spread in the wave packet which should be accounted for.

The exact expression for the energy spread in a wave packet which is Gaussian in momentum space can be written (ignoring factors of  $\hbar^2/2m^*$  for convenience)

$$P(E) = 2\delta^2 e^{-2\delta^2(E+E_0)} I_0(4\delta^2 \sqrt{EE_0}) \quad (3)$$

where  $E_0$  is the central energy and  $I_0$  is a modified Bessel function. The smallest value of the energy of interest in this calculation is that associated with the first conductance step when a typical value of the argument  $4\delta^2 \sqrt{EE_0}$  is large (of order  $10^2$ ). In this situation we may employ an asymptotic expansion of  $I_0$  which yields

$$P(E) \simeq \delta \left( 2\pi \sqrt{EE_0} \right)^{-1/2} e^{-2\delta^2(\sqrt{E} - \sqrt{E_0})^2}. \quad (4)$$

It can be seen that this function is essentially Gaussian in  $\sqrt{E}$  modified by a prefactor which is rather weakly dependent upon  $E$ . A deconvolution of the conductance as a function of energy may be effected with the aid of (4) to give an indication of the residual broadening which can be attributed to the geometry of the point contact. For numerical purposes this deconvolution is achieved by evaluating the convolution of the exact expression (4) with a model step function having parameters to control the position and width of each step.

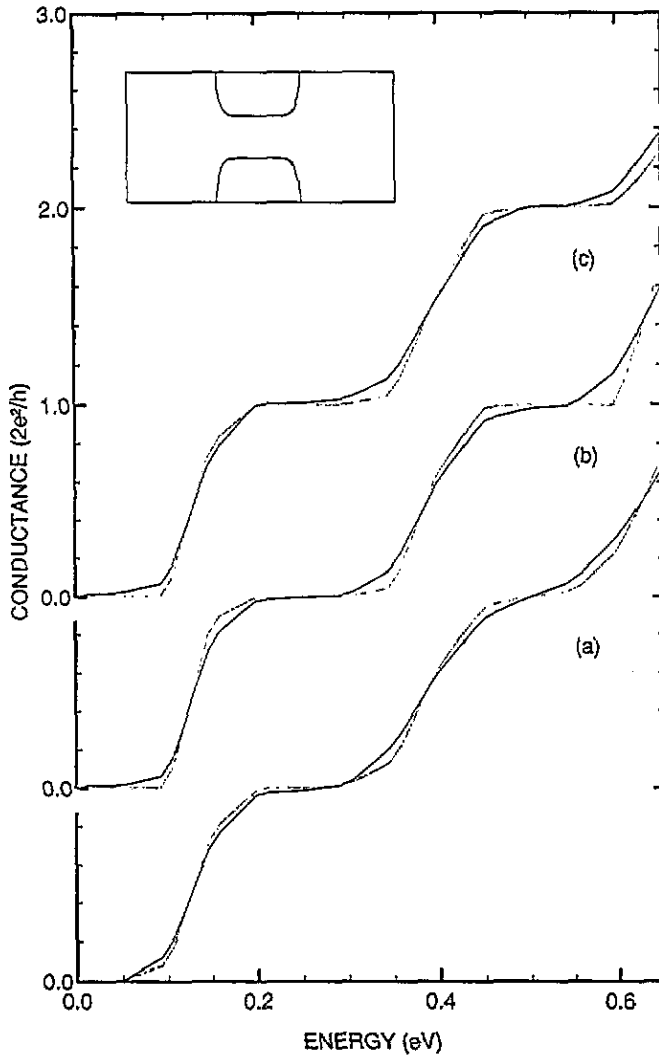


**Figure 1.** Conductance as a function of wave packet energy for systems with length-to-width ratios (a) 3:1, (b) 5:1, and (c) 10:1. The deconvoluted results are also shown (dotted curves) to give an impression of the residual broadening due to the geometry (schematic inset).

The model functions giving the best fit to the numerical results are also shown in figure 1. Comparing the two sets of curves it can be seen that the degree of broadening is not greatly affected, demonstrating that the energy spread of the wave packet has not unduly distorted the results.

As an illustration of the power of the method the effect of placing an obstacle or impurity in the channel is shown in figure 2. The width of the point contact is slightly greater in this case ( $\approx 45 \text{ \AA}$ ) while the length-to-width ratio will be from now on 10:1. A scatterer of finite spatial extent is placed initially at the centre of the channel. The scatterer was chosen to be Gaussian in profile and have a strength large enough to make its presence felt over energies corresponding to the first few conductance steps. As the position of the scatterer in the direction perpendicular to the length of the channel is changed (moved away

from the centre) it affects the conductance in a manner which is dependent upon both the position and the particular step. Close inspection of figure 2 shows that the first and third steps become sharper as the scatterer is moved away from the centre ((a)→(e)) whereas the second step is degraded. This may be understood by a consideration of the form of the transverse bound state wave functions in the absence of the scatterer,  $\phi_n(y)$ . In a long, unobstructed channel the energies of these states would precisely define the step positions. For odd-numbered states, with the lowest being  $n=1$ ,  $|\phi_n(y)|^2$  is large at the centre of the channel, while for even-numbered states  $|\phi_n(y)|^2$  is negligible at the centre. The effect of the scatterer on the quality of a given step is then greatest when the scatterer resides in a position corresponding to a maximum of  $|\phi_n(y)|^2$  and least at a minimum, exactly as seen in figure 2.

The results shown in figure 2 illustrate a further point which should be mentioned at this stage. This is that the accuracy of the quantization in the third step can be seen to be poorer than that of the first and second steps. The cause is an insufficient number of points on the grid to provide a good representation of the more highly modulated wave function associated with the higher harmonics within the confining potential. If desired this can be remedied by taking a smaller grid spacing in the transverse direction.

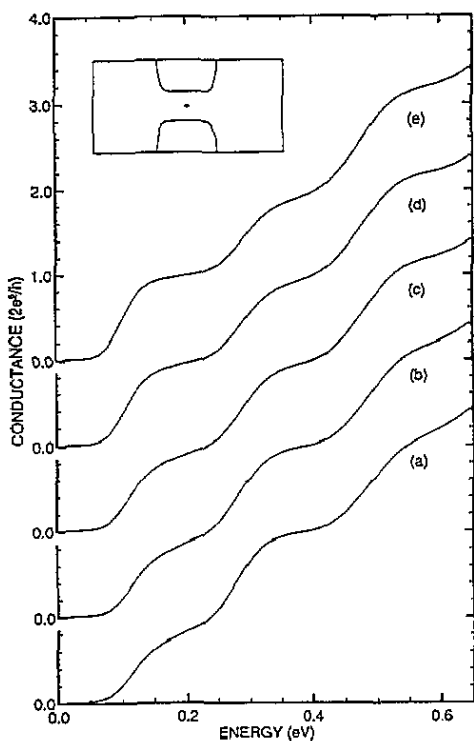


**Figure 2.** A similar geometry with a scattering potential (shown inset) initially at the centre of the channel (a). The position of the scatterer is moved in the direction perpendicular to the length of the channel (away from the centre). The distances are (b) 5 Å, (c) 10 Å, (d) 15 Å, and (e) 20 Å. Note how the effect varies from step to step.

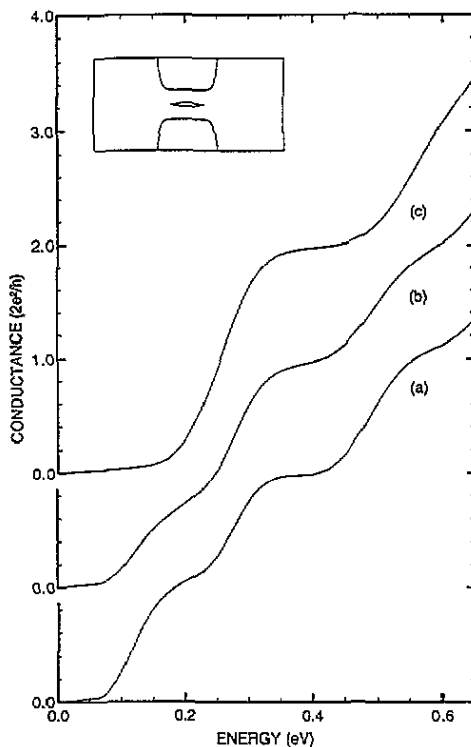


**Figure 3.** The effect of splitting the channel along its central axis with a potential barrier. The ratios of the barrier length to the width of the new channels are approximately (a) 1:2, (b) 1:1, and (c) 4:1. Curve (c) shows clearly the loss of the conductance step at  $2e^2/h$ .

Figure 3 shows the effect of placing a 'partition' of varying length in the centre of the same channel thus creating two narrower channels. As the length of the partition increases compared to that of the width of the new channels, the conductance step at  $2e^2/h$  is lost and is replaced by a single step at twice the original value. This corresponds to a situation which may be thought of as two parallel channels of the same width in each of which the onset of conductance occurs at a higher energy than for the single wider channel. It is found that the transition from quantization at one to two units of  $2e^2/h$  is rapid as the length of the dividing barrier exceeds the width of the new channel, providing the barrier is high enough (the maximum value of the potential corresponding to an energy greater than that of the original conductance steps). This figure could also be described approximately in the terms used to explain figure 2. The second step is little changed throughout because the partition sits at a zero of  $|\phi_2(y)|^2$  while the first and third steps are degraded due to the associated maxima of  $|\phi_1(y)|^2$  and  $|\phi_3(y)|^2$ .

In summary, a numerical method for the calculation of the conductance of point contacts defined by an artificial potential landscape has been outlined. Results for simple model potentials show conductance quantization free of the structure associated with abruptly varying constrictions. The time-dependent method allows realistic potentials to be studied at relatively modest computational expense, the flexibility in the choice of potential giving scope for the study of a diverse range of problems. Furthermore, propagation schemes exist which will allow the inclusion of a magnetic field [15].

The authors gratefully acknowledge helpful discussions with S Holloway. One of us (KS) received financial support from the UK Science and Engineering Research Council while this work was in progress.

## References

- [1] Mohan V and Sathyamurthy N 1988 *Comput. Phys. Rep.* **7** 213
- [2] van Wees B J, van Houten H, Beenakker C W J, Williamson J G, Kouwenhoven L P, van der Marel D, and Foxon C T 1988 *Phys. Rev. Lett.* **60** 848
- [3] Wharam D A, Thornton T J, Newbury R, Pepper M, Ahmed H, Frost J E F, Hasko D G, Peacock D C, Ritchie D A, and Jones G A C 1988 *J. Phys. C: Solid State Phys.* **21** L209
- [4] Kirczenow G 1988 *Solid State Commun.* **68** 715
- [5] Escapa L and Garcia N 1989 *J. Phys.: Condens. Matter* **1** 2125
- [6] Haanappel E G and van der Marel D 1989 *Phys. Rev. B* **39** 5484
- [7] Szafer A and Stone A D 1989 *Phys. Rev. Lett.* **62** 300
- [8] Tekman E and Ciraci S 1989 *Phys. Rev. B* **39** 8772
- [9] Song He and Das Sarma S 1989 *Phys. Rev. B* **40** 3379
- [10] Glazman L I, Lesovik G B, Khmel'nitskii D E, and Shekhter R I 1988 *JETP Lett.* **48** 238
- [11] Nixon J A, Davies J H, and Barranger H U 1991 *Phys. Rev. B* **43** 12 638
- [12] Fleck J A, Morris, J R and Feit M D 1976 *Appl. Phys.* **10** 129
- [13] Feit M D, Fleck J A, and Steiger A 1982 *J. Comput. Phys.* **47** 412
- [14] Landauer R 1957 *IBM J. Res. Dev.* **1** 223
- [15] Stratford K and Beeby J L 1993 *NDR and Instabilities in 2-D Semiconductors* ed B K Ridley, N Balkan and A J Vickers (New York: Plenum) p 385